Analytical Initialization for Three-Dimensional Numerical Models

J. M. FRITSCH, E. L. MAGAZINER AND C. F. CHAPPELL

Atmospheric Physics and Chemistry Laboratory, NOAA, Boulder, CO 80303

(Manuscript received 3 January 1979, in final form 5 March 1980)

ABSTRACT

A technique for generating analytical initial conditions for three-dimensional numerical models is presented. The technique combines trigonometric and other mathematical functions with meteorological constraints to construct an idealized atmosphere which exhibits commonly observed "real" atmosphere structural characteristics. For example, pressure and thermal waves which slope with height, tropopause, low-level moist tongue, phase differences in pressure and thermal waves, and a jet maximum at the tropopause level are all generated by the simple system of equations.

Examples of both mesoscale and synoptic-scale initial conditions are given, and results of integrating the mesoscale initial conditions in a three-dimensional model are shown. The initialization procedure is economical and flexible, and potential applications include testing weather modification sensitivity, finite-difference schemes, lateral boundary formulations, and various subgrid-scale parameterizations.

1. Introduction

In the past 30 years, numerical modeling of the atmosphere has come a long way from the first numerical integration using the barotropic vorticity equation (Charney *et al.*, 1950). Today's hierarchy of numerical schemes includes models for studying boundary-layer processes, calculating the effects of SST's on stratospheric ozone, generating indices for severe weather forecasts, investigating tropical storm and hurricane development, deducing paleoclimatic circulations, predicting short- and long-term as well as finite-area and global-scale weather, incorporating the effects of cumulus ensembles on the large scale, forecasting pollution levels, simulating the general circulation, determining the evolution of high-level frontogenesis, and a host of other even more specialized applications.

Considering the tremendous complexity of mesoscale and synoptic-scale extratropical systems, numerical testing and evaluation of subgrid-scale parameterizations or numerical techniques might be simplified by initializing with a generalized set of analytical initial conditions. This approach would reduce the usual problems associated with real data initialization and the treatment of boundary conditions. In addition, analytical formulation of initial conditions should permit investigation of an arbitrary spectrum of wavelengths, pressure gradients, static stabilities, etc. In the field of weather modification, a capability of arbitrarily varying initial conditions is particularly important, since it is reasonable to expect that the response of some systems to modification forcing will be virtually nil while others might be strongly susceptible to a modification perturbation. In the event that large-scale field experiments become a reality, it would be extremely helpful for case selection to have developed previous insight into the modification sensitivity of a variety of extratropical weather systems.

We have developed a simple procedure for generating analytical initial conditions which may be arbitrarily adjusted to produce a multitude of atmospheric configurations. Basically, the procedure combines trigonometric and other mathematical functions with meteorological constraints (such as the hydrostatic approximation) to construct an idealized atmosphere which exhibits commonly observed "real atmosphere" structural characteristics. For example, pressure and thermal waves which slope with height, tropopause, low-level moist tongue, phase differences in pressure and thermal waves, and a jet maximum at the tropopause level are all generated by the simple system of equations. In the following section we present the mathematical formulation and in Section 3 we show some examples of initial conditions along with the application of these conditions in a numerical model.

2. Mathematical formulation

The initialization procedure first specifies the thermal structure of the atmosphere at all levels along with the pressure at a single level. Using the hydrostatic equation, pressure is then calculated at all other levels. Winds are determined from the geostrophic approximation and then modified by dynamic adjustment.

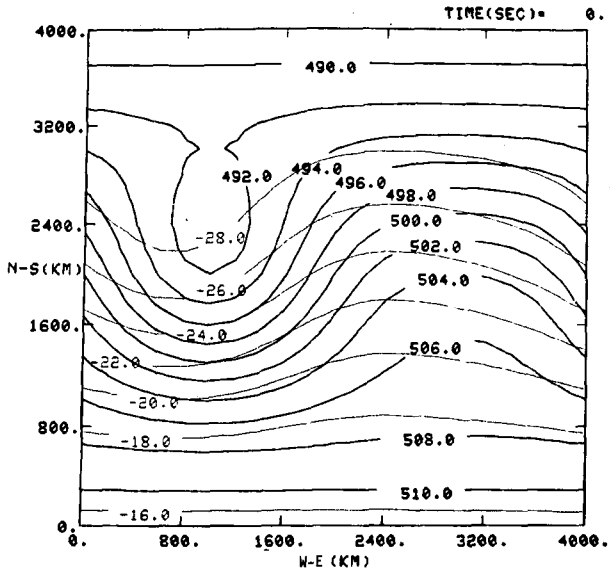

FIG. 1. Synoptic-scale pressure (mb) and temperature (°C) fields at z = 5.57 km (~500 mb level). Dark lines are pressure.

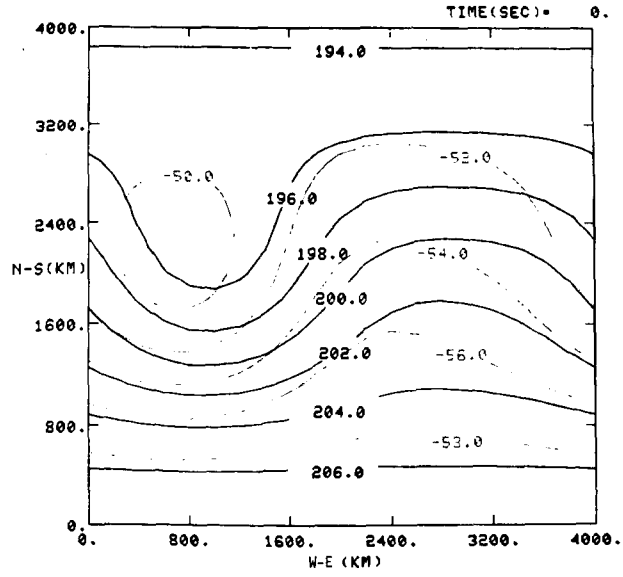

FIG. 3. Synoptic-scale pressure (mb) and temperature (°C) fields at z = 11.78 km (~200 mb level). Dark lines are pressure.

a. Pressure

The pressure field is specified at a single level z_p from which the pressure at all other levels is determined using the thermal field and the hydrostatic equation in the form

$$p(z) = p(z_p) \exp\left(-\frac{g}{R}\bar{T}\Delta z\right), \qquad (1)$$

where $\bar{T}$ is the mean temperature in the layer Δz. Ordinarily, it is convenient to specify the surface pressure or the pressure at some level z_p for which a specific pattern is desired. For example, Fig. 1 shows the pressure specified for the 5.57 km level (≈500 mb). The general expression for the specified pressure field is

$$p(x,y,z_p) = p_0 + \Delta p_y + \Delta p_x, \qquad (2)$$

where

$$\Delta p_y = A_y \sin\left(\frac{\pi y}{L_y} + \frac{\pi}{2}\right), \qquad (3)$$

$$\Delta p_x = A_x C_x G_p(y) \sin\left(\frac{2\pi x}{L_x} + \phi_p\right). \qquad (4)$$

Eq. (2) states that the pressure anywhere on level z_p is simply the sum of a constant (p_0), a north-south perturbation (Δp_y), and an east-west perturbation (Δp_x). By defining the north–south extent of the domain equal to the wavelength (L_y), and adding a ($\pi/2$) phase shift to the sine function, the north-south pressure perturbation produces a pressure field sloping to the north with maximum gradient (and therefore strongest winds) in the center of the domain. The strength of this perturbation is controlled by the amplitude A_y.

Rather than just reflecting a single traveling wave embedded in a zonal current, upper air pressure or height patterns are often the result of many superimposed and interacting waves. By allowing the east-west pressure perturbation to vary both in the east-west and north-south directions, a "multiwave" structure can be created. Further, diffluence areas and jet maxima (such as shown in Figs. 1–4) can then be generated. These wave characteristics are primarily produced by the coefficients $C_x(x)$ and $G_p(y)$, where

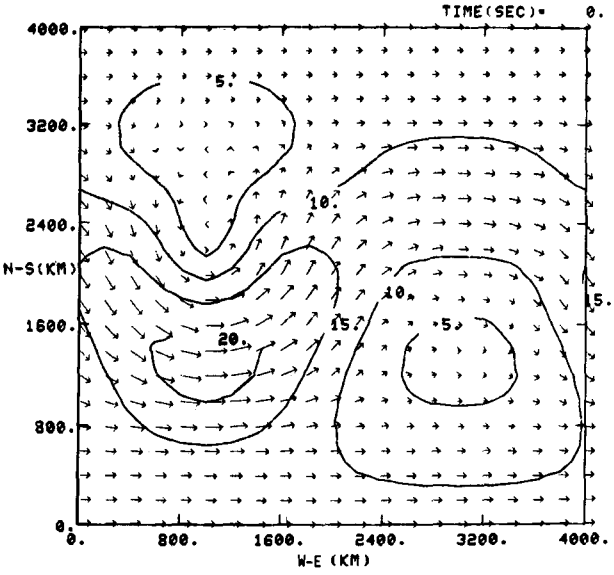

FIG. 2. Synoptic-scale streamline and isotach (m s^{-1}) pattern at z = 5.57 km (~500 mb level).

$$C_x(x) = d_1\left(d_2 + \sin\frac{2\pi x}{L_x}\right), \quad (5)$$

$$G_p(y) = \sin^e\frac{\pi y}{L_y}. \quad (6)$$

For example, setting $d_1 = 1/4$ and $d_2 = 3$ in (5) cuts the pressure perturbation in half from $x = L_x/4$ to $x = 3L_x/4$. Setting $d_1 = 3/8$ and $d_2 = 5/3$ reduces the perturbation by three fourths in the same interval. The north-south change in the east-west perturbation is accomplished through $G_p(y)$. The exponent (e) in (6) allows the gradient to be tightened into a narrow zone. The coefficient A_x in (4) is simply an amplitude constant for the east-west perturbation.

b. Temperature

The development of an expression for temperature follows the same approach as for pressure except that temperature is specified at all levels instead of just the single level z_p. Further, in the real atmosphere, both the phase and amplitude of the thermal wave change with height; thus, the lapse rate must vary in all three dimensions.

A general expression for temperature at any point at any level may be written

$$T(x,y,z) = T_{\text{sfc}}(x,y) + \gamma(x,y,z)\Delta z, \quad (7)$$

where T_{sfc} is the surface temperature and γ is the lapse rate. It is extremely difficult to conceptualize a lapse rate function which will produce realistic three-dimensional structures. Consequently, rather than introduce the three-dimensional variability solely through the lapse rate term, (7) is rewritten in the form

$$T(x,y,z) = T_I(x,y,z) + \gamma(y)\Delta z, \quad (8)$$

where

$$T_I(x,y,z) = T_0 + \Delta T_y + \Delta T_x, \quad (9)$$

$$\Delta T_y = B_y \sin^c\left(\frac{\pi y}{L_y} + \frac{\pi}{2}\right), \quad (10)$$

$$\Delta T_x = B_x C_x(x) D(z) G_T(y) \sin\left[\frac{2\pi x}{L_x} + \phi(z)\right]. \quad (11)$$

Now, it is relatively easy to incorporate realistic vertical variations of thermal waves. For example, the phase term (ϕ) in the sine function in (11) can be adjusted to make the thermal wave slope to the west with height as is frequently observed in synoptic-scale midlatitude disturbances. Similarly, the vertical variation of the amplitude of the east-west thermal wave can be controlled using the function $D(z)$ in (11). For both $\phi(z)$ and $D(z)$, realistic vertical distributions can be obtained from observed midlatitude traveling waves (in order to study a particular type of system), or a spectrum of vertical distributions can be specified for sensitivity testing. Fig. 5 is an example of an observed vertical distribution of $D(z)$. A curve-fitting routine can be applied to the observed data to generate a continuous function such as shown in Fig. 5. Figs. 6–11 show the slope with height of pressure and thermal waves which were initialized for a mesoscale model.

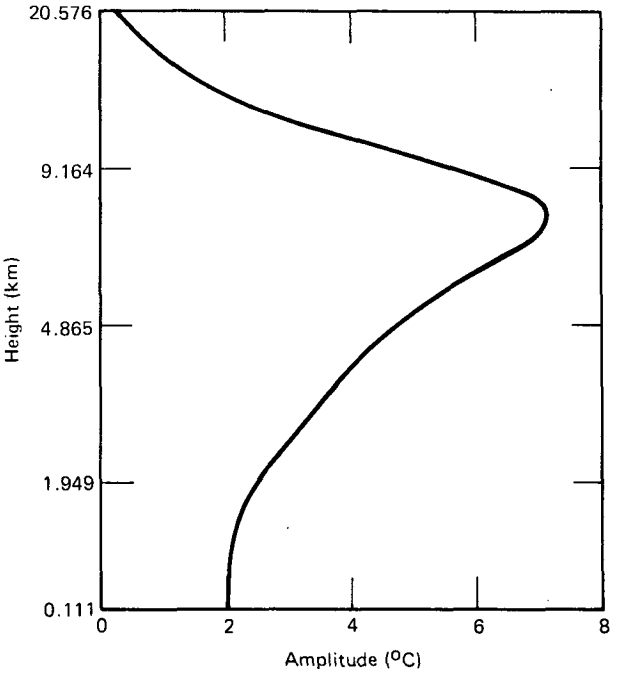

FIG. 5. Change in amplitude of east-west thermal wave as a function of height.

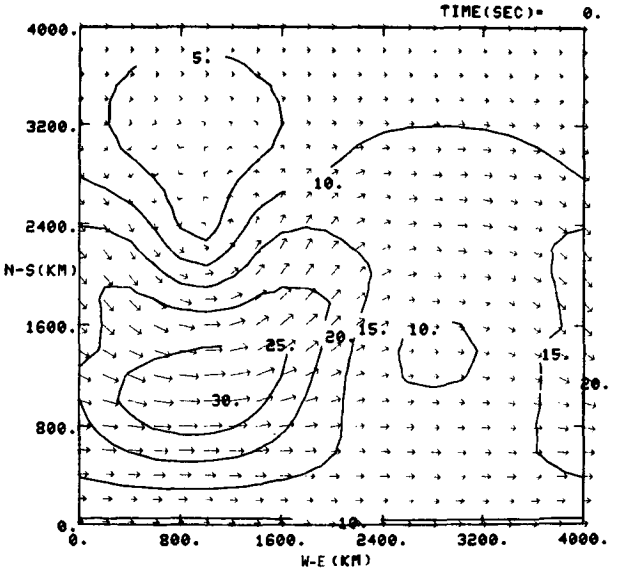

FIG. 4. Synoptic-scale streamline and isotach (m s^{-1}) pattern at z = 11.78 km (~200 mb level).

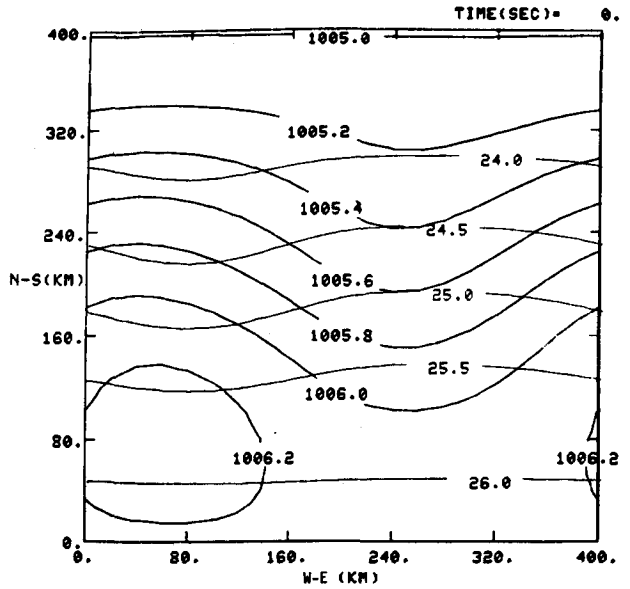

FIG. 6. Mesoscale surface pressure (mb) and temperature (°C) fields. Dark lines are pressure.

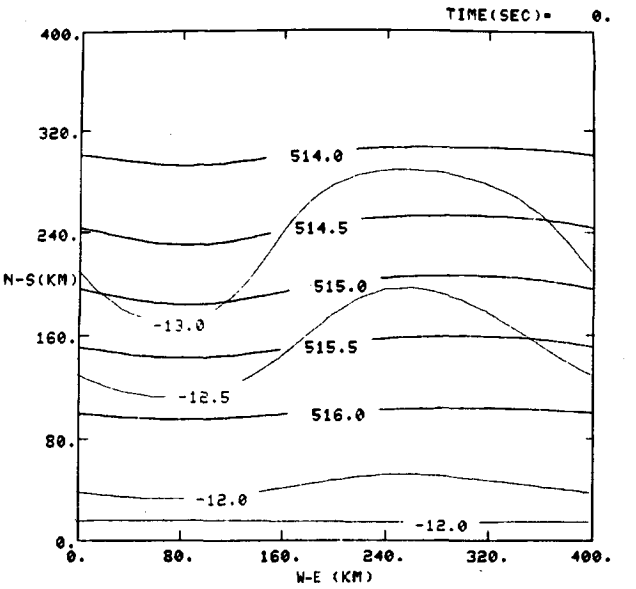

FIG. 8. Mesoscale pressure (mb) and temperature (°C) fields at $z = 5.57$ km (~500 mb level). Dark lines are pressure.

The above formulation could include a north-south vertical variation of the phase by making the constant $(\pi/2)$ phase shift in (10) a function of height. Except for the vertical variation of the amplitude and phase in (11), the roles of the other coefficients and terms in (9), (10) and (11) are the same as described for the pressure in (2) through (6). Thus, the strengths of the north-south and west-east temperature perturbations are controlled by B_y and B_x, respectively. $C_x(x)$ is defined by (5) and $G_T(y)$ is given by

$$G_T(y) = \sin^d \frac{\pi y}{L_y} . \tag{12}$$

As in (6), the exponents in the sine functions in (10) and (12) are used to strengthen or weaken the gradient. In principle, by making the sine function exponent in (12) very large, frontal type gradients can be constructed.

The calculation of the lapse rate in (7) depends

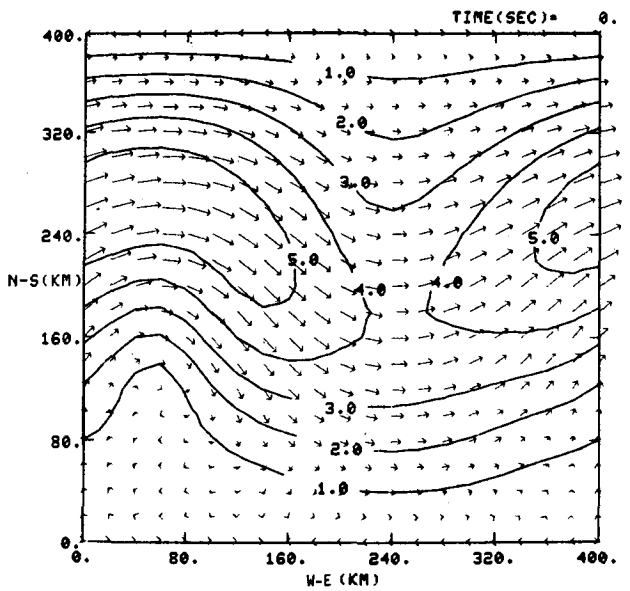

FIG. 7. Mesoscale surface streamline and isotach (m s^{-1}) pattern.

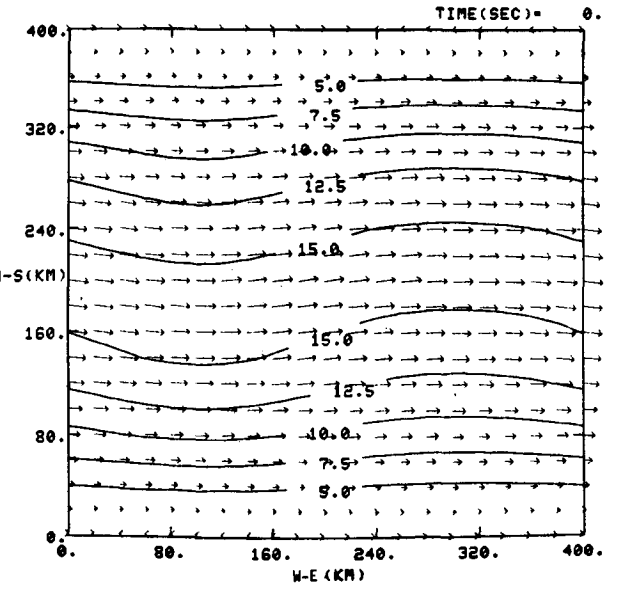

FIG. 9. Mesoscale streamline and isotach (m s^{-1}) pattern at $z = 5.57$ km (~500 mb level).

on whether the troposphere or the stratosphere is being initialized. In the troposphere, $\gamma(y)$ is given by

$$\gamma(y) = \gamma_t + K_t \sin^a \frac{\pi y}{2L_y}, \quad (13)$$

and the stratosphere $\gamma(y)$ is defined by

$$\gamma(y) = \gamma_s + K_s \sin^b \frac{\pi y}{L_y}. \quad (14)$$

The constants K_t and K_s are the amplitudes of the north-south changes in the constant lapse rates (γ_t and γ_s) for the troposphere and the stratosphere, respectively. Once again the exponents of the sine functions are used to determine the gradient.

Upon completion of the definition of the thermal field, lapse rates must be checked for any superadiabatic conditions. Normally, with judicious selection of the lapse-rate constants and slope of the thermal wave, superadiabatic lapse rates are avoided. Fig. 12 is an example of a sounding generated for initializing a mesoscale model used for studying convective systems.

Finally, the height of tropopause (z_t) is related to the thermal wave at an arbitrarily specified height (z_s):

$$z_t = z_s - \frac{\Delta z_t}{B_y} \times [T(x, y = y_0, z = z_s) - T(x, y, z = z_s)], \quad (15)$$

where z_s is the height of the tropopause at the southern boundary, Δz_t is the maximum change in height between the northern and southern boundaries, and B_y is the amplitude of the north-south thermal wave at height z_s. The height of the tropopause, and its north-south variation, are clearly evident in the synoptic-scale example shown in Fig. 13.

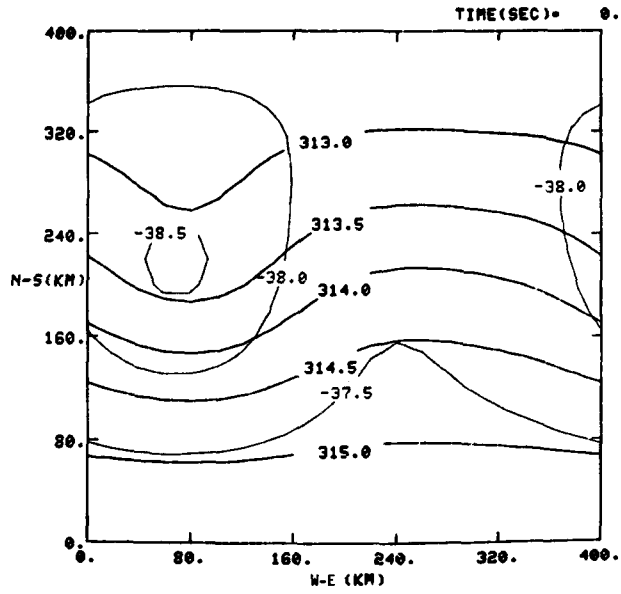

FIG. 10. Mesoscale pressure (mb) and temperature (°C) fields at z = 9.16 km (~300 mb level). Dark lines are pressure.

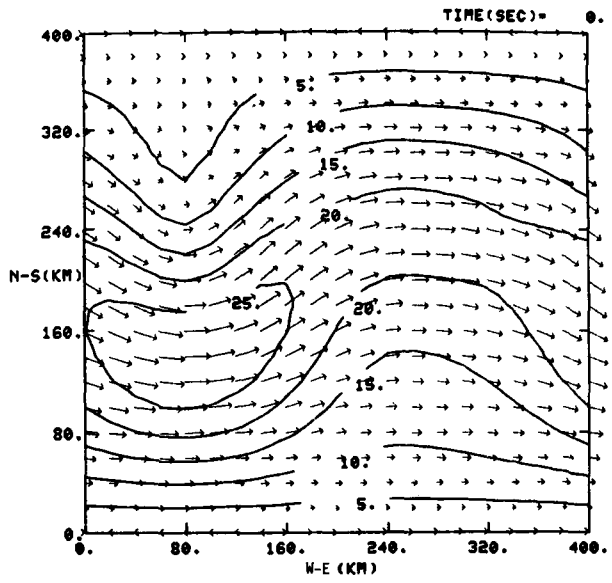

FIG. 11. Mesoscale streamline and isotach (m s^{-1}) pattern at z = 9.16 km (~300 mb level).

c. Wind

A major difficulty in most initialization procedures is achieving a reasonable balance between the pressure or height fields and the wind field. Some large-scale models simply assume geostrophic balance, while others apply the "balance equation" to obtain a more realistic relationship between pressure-surface heights and winds. In multilevel primitive equation models, an alternative method to balance pressure and wind is "dynamic initialization". For analytical initial conditions two steps are involved in the calculation of the initial wind field. A first estimate is obtained from the geostrophic approximation where

$$u = -\frac{RT}{fp}\frac{\partial p}{\partial y}, \quad (16)$$

$$v = \frac{RT}{fp}\frac{\partial p}{\partial x}. \quad (17)$$

This approximation does not produce conditions compatible with the governing primitive equations. Dynamic initialization procedures are designed to produce balanced initial conditions from observed or derived pressure and winds. Basically, these procedures use the model's predictive equations themselves to "nudge" the pressure and wind into balance

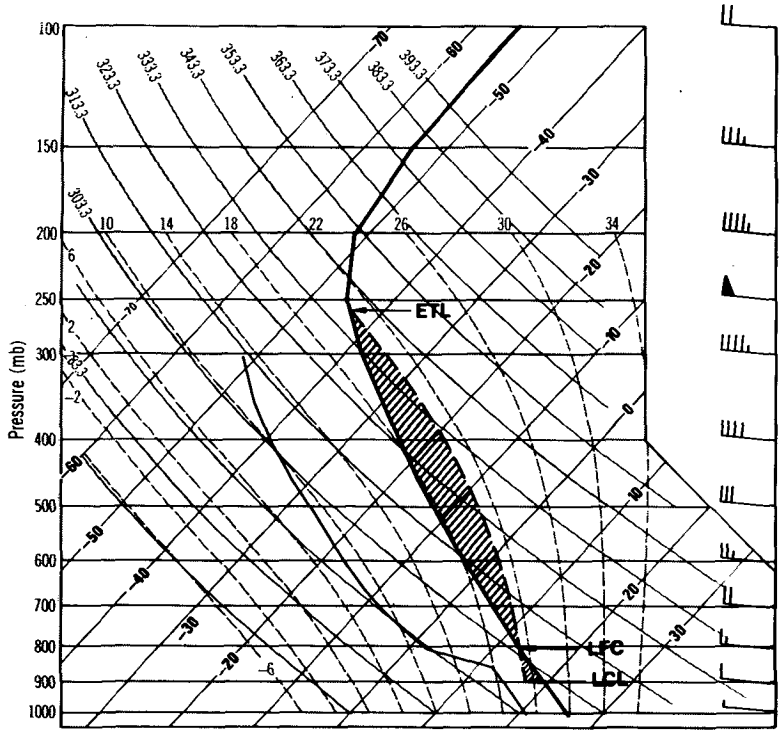

FIG. 12. Sounding of temperature, mixing ratio and wind velocity. Skew $T - \log P$ diagram shows temperature (heavy solid line), mixing ratio (thin solid line) and potential buoyant energy (hatched area). Moist adiabat (dashed line) was constructed for a lifted parcel with mean thermodynamic characteristics of lowest 100 mb layer. Wind barbs are in m s^{-1} where short barb = 2.5, long barb = 5 and flag = 25. LCL is the lifting condensation level, LFC the level of free convection, and ETL the equilibrium temperature level.

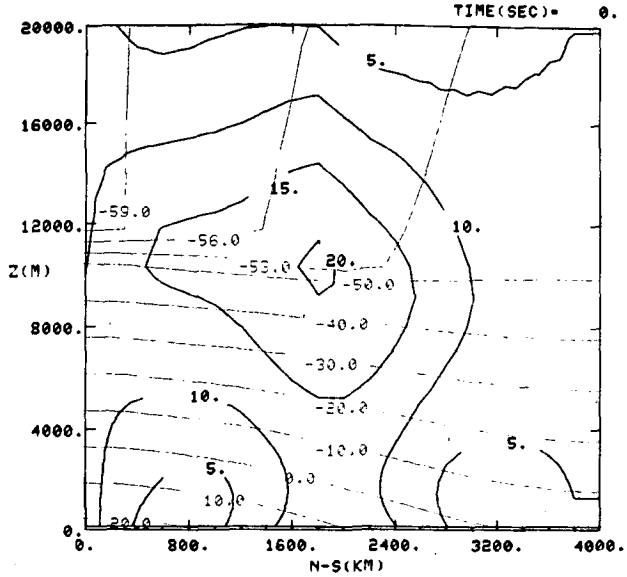

FIG. 13. Synoptic-scale north-south vertical cross-section of wind speed (m s^{-1}) and temperature (°C). Section taken through the east-west center of the domain. Dark lines are wind speed.

before forward integration begins. Hoke and Anthes (1976) have tested one of these procedures and produced a set of initial conditions with less imbalance than other more conventional initialization techniques. However, they point out that their technique is not well-suited for initializing mesoscale disturbances when only temperature and pressure data are available. For the analytical initialization procedure described above, neither observed nor predicted winds are available; only the thermodynamic structure is known. Consequently, the dynamic adjustment scheme developed by Okamura (see Temperton, 1976) has been selected and tested in a model developed by Fritsch and Chappell (1980).

The adjustment procedure consists of a simple cyclic iteration. For example, for the variable α a single iteration is defined by

$$\alpha^* = \alpha^{(\nu)} + \Delta t \left(\frac{\partial \alpha}{\partial t}\right)^{(\nu)}, \tag{18}$$

$$\alpha^{**} = \alpha^* - \Delta t \left(\frac{\partial \alpha}{\partial t}\right)^*, \tag{19}$$

$$\alpha^{(\nu+1)} = 3\alpha^{(\nu)} - 2\alpha^{**}, \qquad (20)$$

where ν is the iteration number and Δt is the time step.

d. Moisture

The initialization of the moisture field is the most arbitrary since for any given wave there are no particular constraints (except saturation) on the water vapor pattern. Of course, some patterns are more reasonable than others depending upon the type of testing to be done. For example, the moisture field described below was designed to test a convective parameterization technique for midlatitude squall-line convection. Consequently, a moist tongue is introduced into the low-level southerly flow. Relative humidity (h) is used as the moisture parameter

$$h = h_0 + \left| h_a \sin \frac{\pi x}{L_x} \right|, \qquad (21)$$

where h_0 is some minimum relative humidity for the entire grid and h_a is defined by

$$h_a = \begin{cases} \dfrac{k}{z}, & z > 1.5 \text{ km} \\ k, & z \leq 1.5 \text{ km}. \end{cases} \qquad (22)$$

In (22) both k and z are specified in km. Fig. 14 shows the initial surface moisture distribution for a mesoscale model where $k = 0.6$ km and $h_0 = 0.2$.

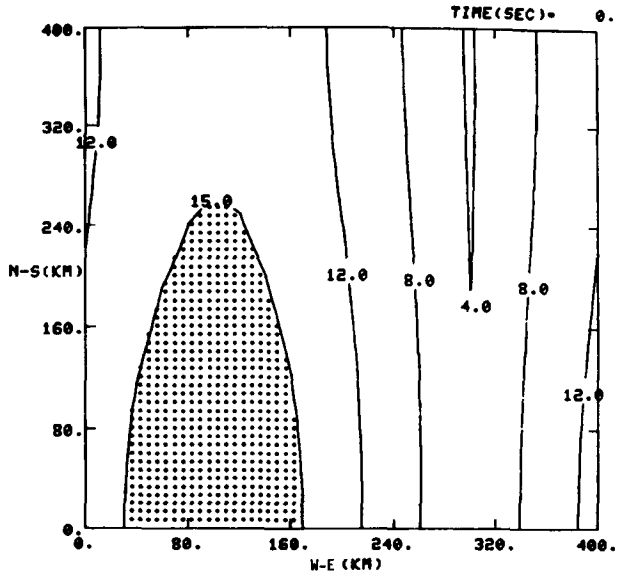

FIG. 14. Mesoscale water vapor mixing ratio (g kg^{-1}) at the surface.

TABLE 1. Constants for generation of mesoscale initial conditions.

Constant	Value	Related physical characteristic or definition
a	3.1	adjusts the north-south gradient of the lapse rate
A_x	0.2	amplitude of pressure wave at reference level
A_y	1.5	amplitude of north-south pressure wave
b	1.0	north-south change in lapse rate
B_x	1.0	amplitude of east-west thermal wave
B_y	1.25	amplitude of north-south thermal wave
c	1.0	adjusts gradient of north-south thermal wave
d	3.0	north-south gradient of east-west thermal wave
d_1	0.25	east-west change in amplitude of east-west thermal wave
d_2	3.0	east-west change in amplitude of east-west thermal wave
e	4.0	north-south gradient of east-west pressure wave on reference level
h_0	20%	minimum relative humidity
k	0.6	amplitude of humidity wave
K_t	0.2	maximum north-south change in tropospheric lapse rate
K_s	0.06	maximum north-south change in stratospheric lapse rate
L_x	400 km	wavelength of east-west thermal and pressure wave
L_y	400 km	wavelength of north-south thermal and pressure wave
p_0	515 mb	reference level pressure at southern boundary
T_0	298 K	surface temperature at southern boundary
z_s	11.78 km	height of tropopause at southern boundary
z_0	0.111 km	height of lowest model level
z_p	5.574 km	reference level where pressure pattern is defined
γ_s	-0.2 C km^{-1}	lapse rate in stratosphere
γ_t	-7.0 C km^{-1}	lapse rate in troposphere
ϕ_0	$\pi/8$	phase of thermal wave at lowest level
ϕ_p	π	phase adjustment of pressure wave at reference level

3. Application of analytical initial conditions to a numerical model

Using a three-dimensional primitive equation model cast in Cartesian coordinates, analytically generated mesoscale initial conditions were tested with a 3 h integration. The initial conditions were generated using the system described in Section 2 and the constants defined in Table 1. The numerical model has constant conditions along the north and south boundaries, and is periodic in the east-west. Horizontal grid resolution is 20 km with 20 levels in the vertical. Diurnal heating at the surface is in-

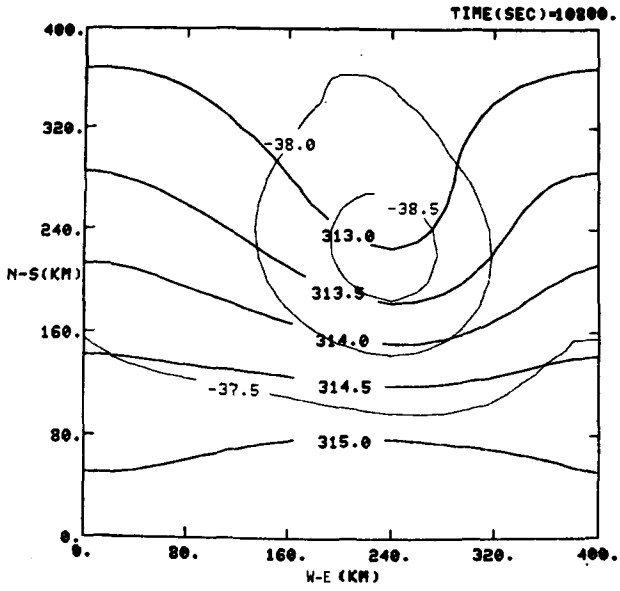

FIG. 15. Mesoscale pressure (mb) and temperature (°C) fields at z = 9.16 km (~300 mb level) for 3 h integration. Dark lines are pressure.

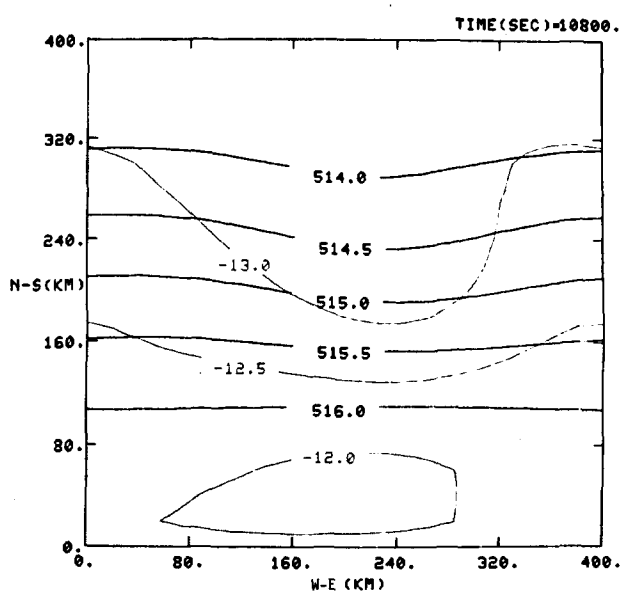

FIG. 17. Mesoscale pressure (mb) and temperature (°C) fields at z = 5.57 km (~500 mb level) for 3 h integration. Dark lines are pressure.

cluded. A complete model description is available in Fritsch and Chappell (1980).

The primary purpose of the numerical integration is to determine if the analytical initial conditions are physically consistent. Evidence for this would be the orderly eastward propagation of the initial wave, without large adjustments or changes in the initial thermodynamic and kinematic patterns. Figs. 15 and 16 show the thermodynamic and kinematic structure at the 9.16 km (~300 mb) level after 3 h of integration. Comparing these figures to the initial conditions in Figs. 10 and 11 indicates that the wave speed is approximately the same as the mean westerly flow. Similarly, at the 5.57 km (~500 mb) level, comparing Figs. 17 and 18 to Figs. 8 and 9 shows the same type of movement and adjustment. At the surface (cf.

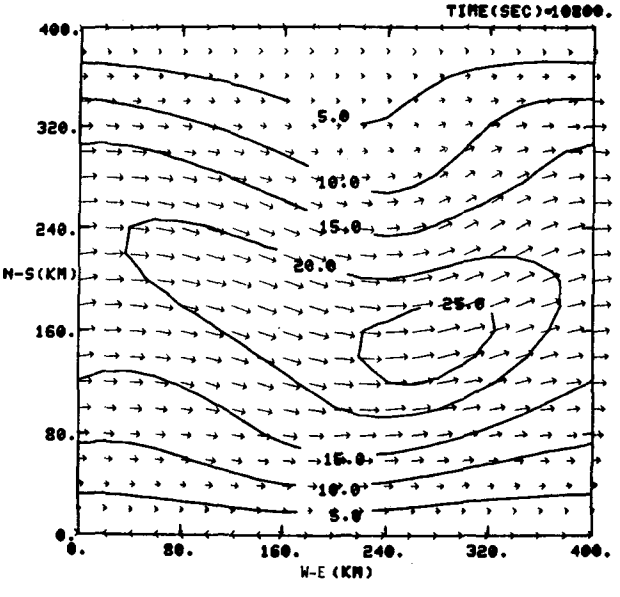

FIG. 16. Mesoscale streamline and isotach (m s^{-1}) pattern at z = 9.16 (~300 mb level) for 3 h integration.

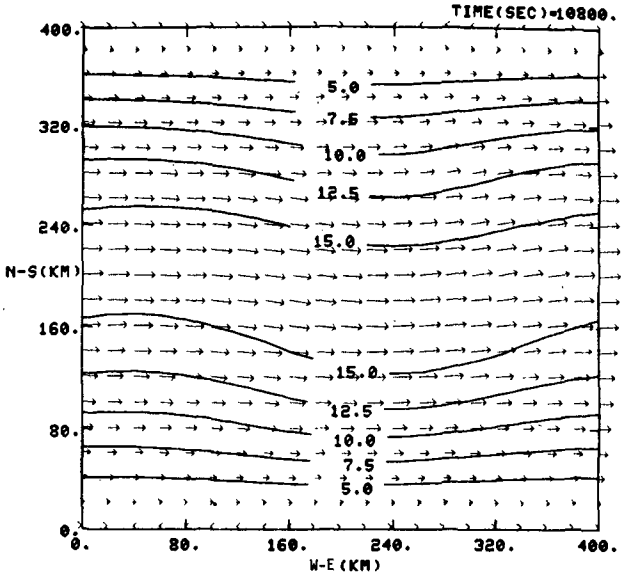

FIG. 18. Mesoscale streamline and isotach (m s^{-1}) pattern at z = 5.57 km (~500 mb level) for 3 h integration.

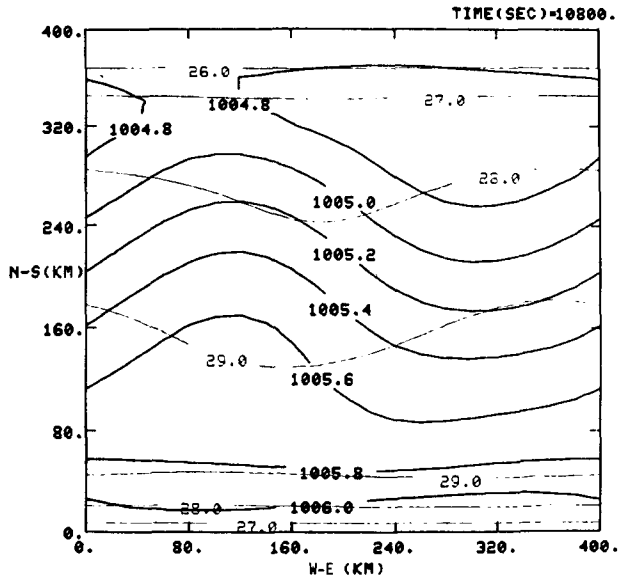

FIG. 19. Mesoscale surface pressure (mb) and temperature (°C) fields for 3 h integration. Dark lines are pressure.

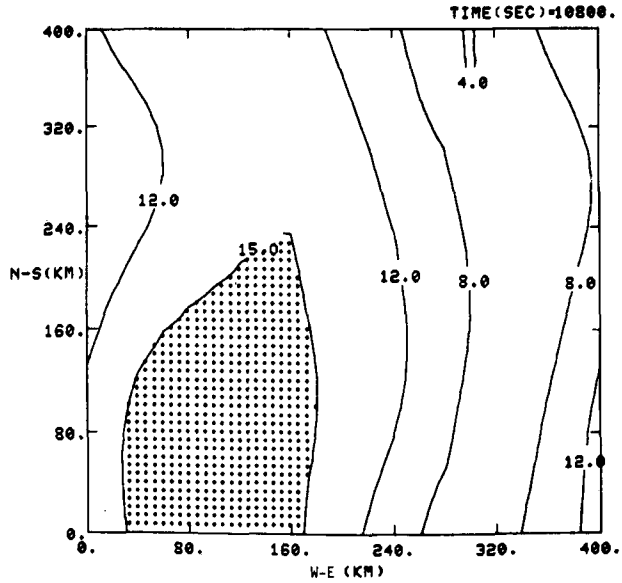

FIG. 21. Mesoscale water vapor mixing ratio (g kg^{-1}) at the surface for 3 h integration.

Figs. 19 and 20 to Figs. 6 and 7), a much larger adjustment is apparent in the thermal field in response to the diurnal heating imposed on the interior of the grid. On the other hand, the surface pressure pattern has slowly propagated eastward without any large distortions. Also, at the surface, the water-vapor mixing-ratio field has shifted eastward in the center of the domain where the surface winds are strongest (cf. Fig. 21 to Fig. 14). Finally, the traveling wave has developed a vertical motion pattern (Fig. 22) consistent with the couplet of warm and cold advection.

Additional numerical integrations were performed on synoptic-scale waves and for mesoscale systems with initial structures different from the systems presented above. Integrations initialized with large-scale waves were integrated for as long as 18 h, while mesoscale systems were tested up to 6 h. In each case, radical changes or large adjustments did not develop.

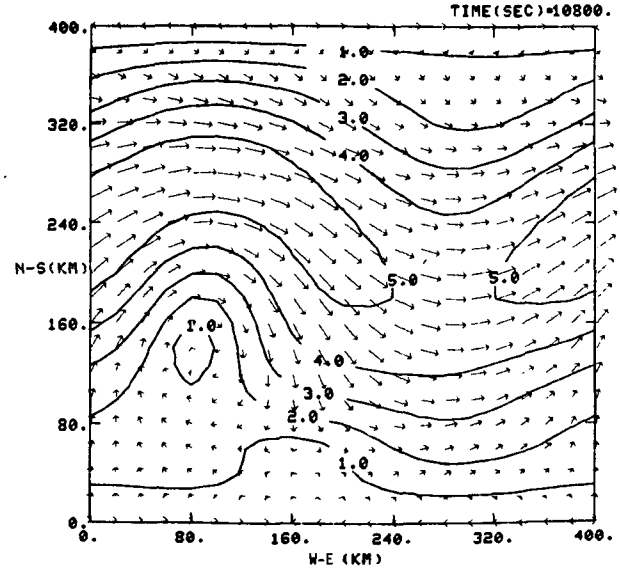

FIG. 20. Mesoscale surface streamline and isotach (m s^{-1}) pattern for 3 h integration.

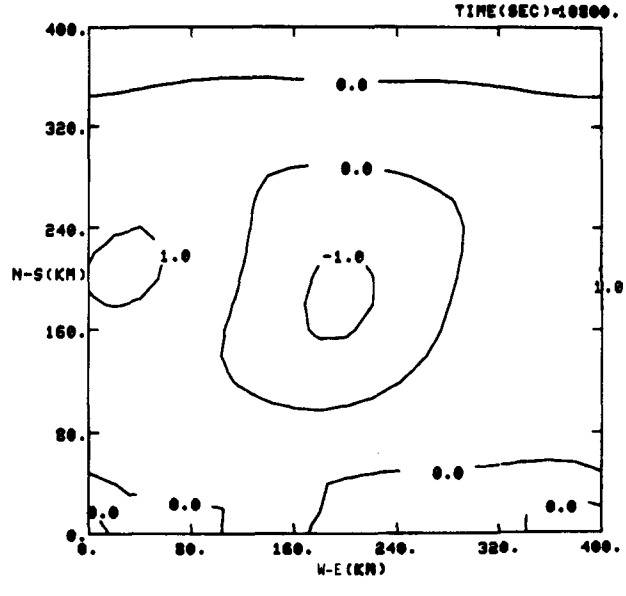

FIG. 22. Mesoscale vertical motion (cm s^{-1}) field at z = 0.988 km (~900 mb level) for 3 h integration.

4. Summary

A technique for analytically generating a physically consistent set of initial conditions for three-dimensional numerical models is defined. The technique combines trigonometric and other mathematical functions with meteorological constraints to produce atmospheres which exhibit characteristics of the real atmosphere. The system of equations is very flexible; it permits the generation of three-dimensional atmospheric structures ranging from the mesoscale through the synoptic.

Potential applications include testing weather modification sensitivity, finite-difference schemes, lateral boundary-condition formulations and subgrid-scale parameterizations. The initialization is economical when compared to obtaining a data set and generating a consistent set of initial conditions by objective analysis: a computer implementation of the procedure runs in less than 13 CPU s on a CDC 6600.

REFERENCES

Charney, J. G., R. Fjørtoft and J. von Neumann, 1950: Numerical integration of the barotropic vorticity equation. *Tellus*, **2**, 237–254.

Fritsch, J. M., and C. F. Chappell, 1980: Numerical prediction of convectively driven mesoscale pressure systems. Part II: Mesoscale model. *J. Atmos. Sci.* (in press).

Hoke, J. E., and R. A. Anthes, 1976: The initialization of numerical models by a dynamic-initialization technique. *Mon. Wea. Rev.*, **104**, 1551–1556.

Temperton, C., 1976: Dynamic initialization for barotropic and multi-level models. *Quart. J. Roy. Meteor. Soc.*, **102**, 297–311.